

Optimizing Designed Variable Speed Control Moment Gyroscopes with Variable Skew Angle

Feng Liu, Feng Gao, Xiaojun Ding

School of Electrical Information Engineering, North Minzu University, Yinchuan, China

Email: address:yctxh101_cc@126.com

How to cite this paper: Liu, F., Gao, F. and Ding, X.J. (2023) Optimizing Designed Variable Speed Control Moment Gyroscopes with Variable Skew Angle. *Journal of Applied Mathematics and Physics*, 11, 3315-3344. <https://doi.org/10.4236/jamp.2023.1111212>

Received: August 21, 2023

Accepted: November 4, 2023

Published: November 7, 2023

Copyright © 2023 by author(s) and Scientific Research Publishing Inc. This work is licensed under the Creative Commons Attribution International License (CC BY 4.0).

<http://creativecommons.org/licenses/by/4.0/>



Open Access

Abstract

Large torque can be output by the single gimbal control momentum gyroscope (SGCMG) based on the principle of the gyroscopic precession. However, the singularity is a major obstacle to successfully implement the task of the attitude control. The singularity can be avoided by the additional variable flywheel speed of variable speed control moment gyroscopes (VSCMG). Unfortunately, some kind of singularity cannot be effectively avoided. Consequently, the output torque can be only supported by the reaction torque of the flywheel when the singularity is encountered, and the consume power that is determined by the flywheel speed and reaction torque can be greatly increased when the flywheel spin rate over one thousand revolutions per minute. In this paper, the pyramid configuration with variable skew angle of the VSCMG is considered. A new steering law for the VSCMG with variable skew angle is proposed. The singularity that cannot be avoided by the varying flywheel speed can be effectively avoided with assisting of varying the skew angle. Consequently, the requirement of flywheel torque can be reduced. At last, the optimizing VSCMG with variable skew angle can be cast as a multi-objective function with multi-constraints. The particle swarm optimization method is used to solve the optimizing problem. In summary, the VSCMG with variable skew angle can be redesigned with considering of the singularity avoidance and minimizing system power.

Keywords

VSCMG, Pyramid Configuration with Variable Skew Angle, New Steering Law Designed, Optimization Parameters

1. Introduction

The large torque can be output by the varying gimbals position of the single gimbal control momentum gyroscopes (SGCMG) [1] [2]. The torque amplifi-

cation performance can be possessed by the SGCMG based on the theory of the gyroscope precession principle [2]. Unfortunately, the output torque of the SGCMG cannot be supported by the gyroscopic torque when singularity is encountered [3]. The singularity is the mainly obstacle in successfully operating the attitude control task [4]. The singularity can be effectively avoided by assisting of the varying flywheel spin rate of the variable speed control momentum gyroscopes (VSCMG) [1] [4].

Compared with single gimbal control momentum gyroscopes (SGCMG), the singularity can be avoided by assisting the variable spin rate of the VSCMG [4]. Unfortunately, according to analyze of the recent reports, some singularity cannot be avoided even by assisting the variable spin rate. Consequently, the output torque of the VSCMG can be supported only by the reaction torque of the flywheels when the singularity is encountered, and the flywheel torque can be greatly increased [4]. So the flywheel power that is determined by the flywheel torque and flywheel speed can be greatly increased when the flywheel spin rate reaching to thousands revolutions per minute [5] [6] [7] [8].

In order to effectively avoid the singularity, the additional freedom should be added in the VSCMG. In this paper, the variable skew angle is added in the VSCMG. The variable skew angle is first introduced in the Ref. [9] for the SGCMG.

According to analyze of the Ref. [9], the singularity characteristics cannot be changed with varying skew angel. Consequently, steering skew angle does not seem to help avoidance singularity. Fortunately, the output torque can also be output by the varying skew angle. So null motion can be reconstructed and the singularity can be effectively avoided. Although, the ability of singularity avoidance can be increased by varying skew angle, the additional hardware should be added and the additional consume power should be added, which is not suitable for aerospace application with low power consume [10]. Consequently, optimization designed of the VSCMG with variable skew angle with minimizing power need to be further analyzed.

The optimization design of the VSCMG for pyramid configuration with fixing skew angle has already been proposed in the Ref. [1] and Ref. [8] with minimum flywheel rotational inertia and flywheel power. The additional torque can be output with varying skew angle. So the requirement of the flywheel torque will be reduced by the skew angle when the singularity is encountered [8] [9] [10]. According to above analysis results, in order to further reduce the flywheel torque, the pyramid configuration of the VSCMG with variable skew angle need to be considered. The purpose of introducing the variable skew angel is used for singularity avoidance. Unfortunately, the steering skew angle in the new designed steering law is not considered. So the new steering law needed to be further studied.

In order to optimize design of the VSCMG with variable skew angle, the following two parts should be given. The first one is that the exchangeable angular momentum envelop for the VSCMG with variable skew angle should be further

analyzed. The other one is that the new steering law with minimizing flywheel torque for the VSCMG with variable skew needed to be redesigned. The angular momentum envelop of the VSCMG with fixing skew angle have already been analyzed in Ref. [11] and Ref. [12]. The characteristics of the exchangeable angular momentum for the VSCMG with variable skew angle have not been reported. At the same time, the designed steering law for VSCMG with fixing skew angle has already been extensively studied [13]-[18]. However, the designed steering law for VSCMG with variable skew angle has not been reported.

According to the principle of the gyroscopic precession, the direction of the gyroscopic torque of the one unit is perpendicular to the angular momentum vector. At the same time, the gyroscopic torque of the one unit is perpendicular to the vector of the gimbal axis. So the direction of the gyroscopic torque of the SGCMG with only one unit will be varied when the gimbal position is varying. Consequently, the multi-units of the SGCMG will be needed for the torque requirement with three-dimensional space. For the system of the SGCMG, the more number of the units, the stronger ability of the singularity avoidance can be achieved. However, considering the mass and power constraints of the space application requirements, the less number of elements in the configuration would be a better choice. Consequently, the singularity problem will become more serious. The designed configuration for the SGCMG with minimizing unit should be balanced between the singularity avoidance and the power and mass. According to analyze the pre-existed works, the pyramid configuration has a unit redundancy, the singularity can be avoided, and the torque with three-dimensional torque can be output. In additional, it is the simplest configuration of the actuator of the attitude control system, and it has already been widely used in the attitude control system of the spacecraft. Furthermore, the singularity analysis with different configuration can be guided and provided by the pre-existed analysis results of the pyramid configuration. The VSCMG with variable degree of the flywheel speed and variable degree of the skew angle are still working in the mode of the SGCMG in the most majority of the time. According to above analysis results, the configuration of the VSCMG with variable skew angle will be fixed as pyramid configuration in this paper. The exchangeable angular momentum envelop for VSCMG with variable skew angle is analyzed. The new designed steering law is given under the condition of singularity avoidance and flywheel speed equalization with minimizing flywheel power for the VSCMG with variable skew angle. The optimization parameters of VSCMG with variable skew angle are given under the consideration of singularity avoidance and minimizing whole system power.

Exchangeable Angular Momentum Envelop of VSCMG with Variable Skew Angle

1) System Description

The task of three axis attitude control cannot be only satisfied by one unit of the VSCMG. The three units are the minimum requirement for three axis atti-

tude control. The four units VSCMG with pyramid configuration are frequently used under the considering of system redundancy requirements. In this paper, the pyramid configuration is considered. The system description with pyramid configuration can be expressed as the **Figure 1**. Where β is the skew angle of the pyramid configuration. $\mathbf{g}_i (i=1,2,3,4)$ is the gimbal-axis vector, $\mathbf{g}_1 = s\beta\mathbf{i} + c\beta\mathbf{k}$, $\mathbf{g}_2 = s\beta\mathbf{j} + c\beta\mathbf{k}$, $\mathbf{g}_3 = -s\beta\mathbf{i} + c\beta\mathbf{k}$, $\mathbf{g}_4 = -s\beta\mathbf{j} + c\beta\mathbf{k}$, where, $c\beta = \cos\beta$, $s\beta = \sin\beta$. The net angular momentum vector of the VSCMG can be expressed in spacecraft reference frame (x, y, z) with a set of orthogonal unit vectors $(\mathbf{i}, \mathbf{j}, \mathbf{k})$ as follows.

$$\begin{aligned} \mathbf{H} &= \mathbf{h}_1 + \mathbf{h}_2 + \mathbf{h}_3 + \mathbf{h}_4 \\ &= J\Omega_1 \begin{bmatrix} -c\beta s\delta_1 \\ c\delta_1 \\ s\beta s\delta_1 \end{bmatrix} + J\Omega_2 \begin{bmatrix} -c\delta_2 \\ -c\beta s\delta_2 \\ s\beta s\delta_2 \end{bmatrix} + J\Omega_3 \begin{bmatrix} c\beta s\delta_3 \\ -c\delta_3 \\ s\beta s\delta_3 \end{bmatrix} + J\Omega_4 \begin{bmatrix} c\delta_4 \\ c\beta s\delta_4 \\ s\beta s\delta_4 \end{bmatrix} \end{aligned} \tag{1}$$

where \mathbf{H} is the net angular momentum vector. \mathbf{h}_i is the angular momentum vector and it can be assumed as $s_i = \mathbf{h}_i / J\Omega_i$, and we can get $|s_i| = 1$. J is the inertia of flywheel, Ω_i is the flywheel speed, δ_i is the gimbal position.

In system of the VSCMG with variable skew angle, angular momentum can be exchanged between the spacecraft and the actuator (VSCMG with variable skew angle). In another words, the output torque of the VSCMG with variable skew angle can be output by varying angular momentum.

$$\boldsymbol{\tau}_c = \frac{d\mathbf{H}}{dt} \tag{2}$$

where $\boldsymbol{\tau}_c$ can be denoted as output torque of VSCMG with variable skew angle for attitude control.

The variable angular momentum of the actuator can be caused by three variables: gimbal position, flywheel speed and skew angle. Consequently, the

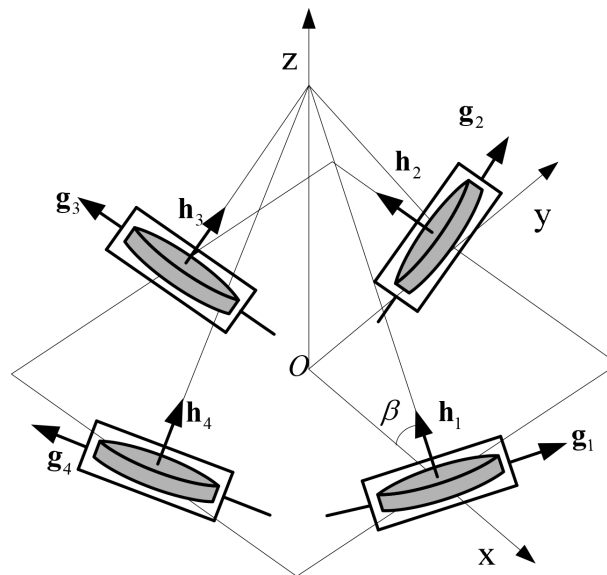


Figure 1. The pyramid configuration of VSCMG.

gyroscopic torque can be output by varying gimbal position, the reaction torque can be output by varying spin rate, and the additional torque that can be output by varying skew angle. The net torque of the VSCMG with variable skew angle can be expressed as follows.

$$\tau_c = \sum_{i=1}^4 \frac{\partial h_i}{\partial \delta_i} \dot{\delta} + \sum_{i=1}^4 \frac{\partial h_i}{\partial \Omega_i} \dot{\Omega} + \sum_{i=1}^4 \frac{\partial h_i}{\partial \beta} \dot{\beta} \tag{3}$$

where $\delta = [\delta_1 \ \delta_2 \ \delta_3 \ \delta_4]^T$, $\Omega = [\Omega_1 \ \Omega_2 \ \Omega_3 \ \Omega_4]^T$, first-order derivative of δ and Ω are the gimbals speed vector $\dot{\delta} = [\dot{\delta}_1 \ \dot{\delta}_2 \ \dot{\delta}_3 \ \dot{\delta}_4]^T$, flywheels acceleration vector $\dot{\Omega} = [\dot{\Omega}_1 \ \dot{\Omega}_2 \ \dot{\Omega}_3 \ \dot{\Omega}_4]^T$, respectively. We can get $\frac{\partial H}{\partial \beta} = [E_1, E_2, E_3]^T$, and $E_1 = Js\beta(\Omega_1 s \delta_1 - \Omega_3 s \delta_3)$, $E_2 = Js\beta(\Omega_2 s \delta_2 - \Omega_4 s \delta_4)$, $E_3 = \sum_{i=1}^4 J\Omega_i c \beta s \delta_i$, $c = \cos$, $s = \sin$. Equation (3) can be rewritten as following matrix form.

$$\tau_c = C\dot{\delta} + D\dot{\Omega} + E\dot{\beta} \tag{4}$$

where $\partial H / \partial \delta = C$, and $\partial H / \partial \Omega = D$ are the Jacobi matrix of gimbals and flywheel, respectively. The specific form can be shown as matrix follows.

$$C = J \begin{bmatrix} -c\beta c\delta_1\Omega_1 & s\delta_2\Omega_2 & c\beta c\delta_3\Omega_3 & -s\delta_4\Omega_4 \\ -s\delta_1\Omega_1 & -c\beta c\delta_2\Omega_2 & s\delta_3\Omega_3 & c\beta c\delta_4\Omega_4 \\ s\beta c\delta_1\Omega_1 & s\beta c\delta_2\Omega_2 & s\beta c\delta_3\Omega_3 & s\beta c\delta_4\Omega_4 \end{bmatrix} \tag{5a}$$

$$D = J \begin{bmatrix} -c\beta s\delta_1 & -c\delta_2 & c\beta s\delta_3 & c\delta_4 \\ c\delta_1 & -c\beta s\delta_2 & -c\delta_3 & c\beta s\delta_4 \\ s\beta s\delta_1 & s\beta s\delta_2 & s\beta s\delta_3 & s\beta s\delta_4 \end{bmatrix} \tag{5b}$$

where $E = \begin{bmatrix} E_1 & 0 & 0 & 0 \\ E_2 & 0 & 0 & 0 \\ E_3 & 0 & 0 & 0 \end{bmatrix}$, $\dot{\beta} = \dot{\beta}[1,1,1]^T$, the first-order derivative of β is spin rate of skew angle.

2) Singularity Analysis

Singularity can be described as follows. Gyroscopic torque can be output in the plane Γ by all units of VSCMG. The output torque cannot be supported by the gyroscopic torque when the direction of the output torque is along the direction that is perpendicular to the plane Γ (Figure 2). In another words, the output torque cannot be supported by the gyroscopic torque when the singularity is encountered.

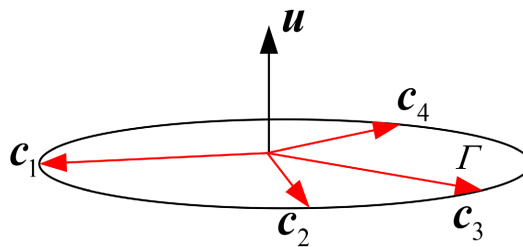


Figure 2. The spatial distribution of gyroscopic torque when singularity is encountered.

Where $c_i (i = 1, 2, 3, 4)$ is unit vector that is column $i (i = 1, 2, 3, 4)$ of matrix C . The gyroscopic torque of each unit can be expressed as vector of c_i . In another word, $c_i (i = 1, 2, 3, 4)$ is the direction along the gyroscopic torque. The singular gimbal positions can be defined as follows: the current gimbal positions can be defined as the singular gimbal positions when the singularity is encountered. In another words, the current gimbal will be staying at the singular gimbal positions when the singularity is encountered. The SGCMG singularity surface can be obtained when taking the gimbal positions over solution space. The singularity direction of the SGCMG singularity can be defined as follows [19] [20].

$$S = \{u : |u| = 1, u \neq \pm g_i, i = 1, 2, 3, 4\} \tag{6}$$

where S is a set of SGCMG singular direction. The vector u of S in the coordination (O-xyz) can be expressed as follows [19] [20].

$$u = s\theta_2 i - s\theta_1 c\theta_2 j + c\theta_1 c\theta_2 k \tag{7}$$

where $s\theta_j = \sin \theta_j$, $c\theta_j = \cos \theta_j$, $j = 1, 2$. θ_1 and θ_2 are the rotation angle along the x axis and y axis, respectively. We can get $\theta_1 \in [0^\circ, 360^\circ]$, $\theta_2 \in [0^\circ, 360^\circ]$. The following equation can be obtained based on the principle of the gyroscopic precession [19] [20].

$$c_i = -g_i \times s_i \tag{8}$$

Consequently, the singularity condition can be rewritten as follows.

$$c_i \cdot u = (-g_i \times s_i) \cdot u = 0 \tag{9}$$

According to above analysis results, the output torque of the VSCMG with variable skew angle can be obtained by the variable angular momentum of the four units. Consequently, Equation (9) can be rewritten as follows.

$$dH_G \cdot u = 0 \tag{10}$$

where dH_G is variable angular momentum of the four units with variable gimbal positions when the SGCMG singularity is encountered. The direction of the gyroscopic torque of the VSCMG can be expressed as following equation when the gimbal staying at singular gimbal positions.

$$c_i = \mp \frac{g_i \times u}{|g_i \times u|} \tag{11}$$

According to the principle of the gyroscopic precession, the vector of flywheel angular momentum can be expressed with cross of the vector of the gyroscopic torque and gimbal axis.

$$s_i = -c_i \times g_i \tag{12}$$

Consequently, the vector of the flywheel angular momentum can be rewritten as following equation with combining Equation (11) and Equation (12).

$$s_i = \pm \frac{(g_i \times u) \times g_i}{|g_i \times u|} \tag{13}$$

The sum angular momentum of the VSCMG with the four units can be shown as following equation when the gimbals staying at singular gimbals positions.

$$\mathbf{H} = \sum_{i=1}^4 \varepsilon_i \frac{(\mathbf{g}_i \times \mathbf{u}) \times \mathbf{g}_i}{|\mathbf{g}_i \times \mathbf{u}|} \quad (14)$$

where $\varepsilon_i = \text{sign}(\mathbf{s}_i \cdot \mathbf{u})$.

The singularity surface can be achieved by Equation (14) when taking θ_1 and θ_2 over $[0^\circ, 360^\circ]$, respectively. According to analysis of Equation (14), the SGCMG singular surface can be classified into 0H singular surface, 2H singular surface and 4H singular surface with different sign of the ε_i [20]. The shape of the singular surface can be varied with variable skew angle.

In the VSCMG system, the variable flywheel speed can be used to avoid the SGCMG singularity. The requirement torque for the task of the attitude control can be only provided by the flywheels when gimbals staying at SGCMG singular gimbals positions and the torque requirement is along the \mathbf{u} . so the projection of each flywheel angular momentum in the \mathbf{u} can be deduced and can be shown as following equation.

$$\mathbf{s}_i \cdot \mathbf{u} = \pm \frac{(\mathbf{g}_i \times \mathbf{u}) \times \mathbf{g}_i}{|\mathbf{g}_i \times \mathbf{u}|} \cdot \mathbf{u} = \pm |\mathbf{g}_i \times \mathbf{u}| \quad (15)$$

Based on the definition of the set \mathcal{S} , we can get $\mathbf{u} \neq \pm \mathbf{g}_i$ ($i=1,2,3,4$). Consequently, we can get $\mathbf{s}_i \cdot \mathbf{u} \neq 0$. The following conclusion can be achieved when the gimbals staying at singular gimbals positions for the VSCMG with variable skew angle. In summary, the following conclusion can be achieved.

$$\text{rank}[\mathbf{C} \quad \mathbf{D} \quad \mathbf{E}] \equiv 3 \quad (16)$$

According to the analyze Equation (16), we can get the conclusion that there is no internal singularity problem in the VSCMG with variable skew angle. In another words, the output torque with three dimensions can be always output weather singularity is encountered or not.

3) The exchangeable angular momentum envelop

The total angular momentum envelop of the VSCMG can be exchangeable between the spacecraft and the actuator. Consequently, the exchangeable angular momentum envelop of the VSCMG can be extended to the maximum angular momentum envelop. The maximum angular momentum envelop of the VSCMG approximate to ellipsoid when $\Omega \in [0, \Omega_{\max}]$, where Ω_{\max} is the up bound of the flywheel spin rate [5].

The maximum angular momentum envelop of the VSCMG is given in Ref. [6] when the flywheel regulation speed have upper and lower bound limitation. There is no gyroscopic torque when the flywheel speed is zero with varying gimbals positions. Besides, the performance of the torque amplification will be deteriorated when the flywheel speed is too low. In addition, any actually system has power limitation. Consequently, the flywheel speed of the VSCMG should have upper bound limitation and lower bound limitation. Ω_{\min} can be marked

as the lower bound limitation of the flywheel speed, Ω_{\max} can be marked as the upper bound limitation of the flywheel speed. The maximum angular momentum envelop of the VSCMG with variable skew angle is given in the following section. The characteristics of the exchangeable angular momentum envelop of the VSCMG with variable skew angle is analyzed.

4) The maximum angular momentum envelop when $\beta \in (0^\circ, 90^\circ)$

The cut section of the angular momentum envelop of the VSCMG with upper and lower bound of flywheel regulation speed can be shown in **Figure 3** when $\beta \in (0^\circ, 90^\circ)$.

In **Figure 3**, *MTRS* can be denoted as angular momentum profile when $\Omega_i = \Omega_{\min}$ ($i = 1, 2, 3, 4$). $\Omega_i \in [\Omega_{\max}, \Omega_{\min}]$ is the flywheel speed ($i = 1, 2, 3, 4$). *GBNA* can be denoted as angular momentum profile when $\Omega_i = \Omega_{\max}$ ($i = 1, 2, 3, 4$). *AEBN* can be denoted the increased angular momentum with regulating flywheel speed. *A* and *B* are the intersections between 4H singular surface and 2H singular surface. *S* and *T* are the intersections between 4H singular surface and 2H singular surface. *N* and *E* are the intersections between 2H singular surface and \mathbf{g}_1 . The net angle momentum of the VSCMG can be expressed as follows.

$$\mathbf{H} = \sum_{i=1}^4 \frac{(\mathbf{g}_i \times \mathbf{u}) \times \mathbf{g}_i}{|\mathbf{g}_i \times \mathbf{u}|} J \Omega_i \tag{17}$$

There is no gyroscopic torque along the \mathbf{u} direction when the gimbals staying at singular gimbal positions. The net angular momentum of the VSCMG with four flywheels angular momentum can be expressed as follows.

$$\mathbf{H} = \sum_{i=1}^4 \mathbf{h}_i = J \sum_{i=1}^4 \Omega_i \mathbf{s}_i \tag{18}$$

where \mathbf{s}_i ($i = 1, 2, 3, 4$) is the unit vector of each flywheel angular momentum. Where $\Omega_i(t)$ ($i = 1, 2, 3, 4, \Omega_i \in [\Omega_{\min}, \Omega_{\max}]$) is the flywheel speed.

The projection of the VSCMG momentum in \mathbf{u} can be expressed as follows.

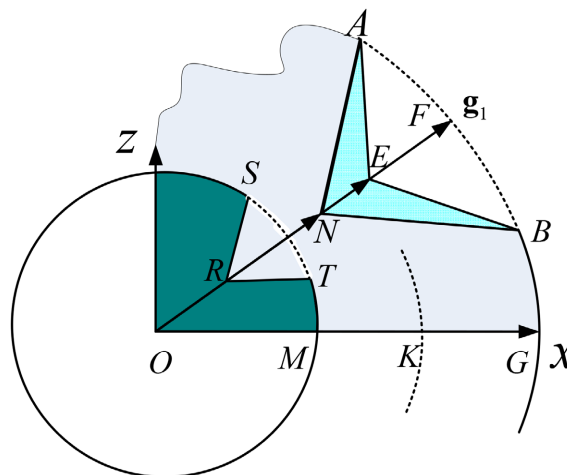


Figure 3. The cut section of the angular momentum profile.

$$J_H = \mathbf{H} \cdot \mathbf{u} = \sum_{i=1}^4 (\mathbf{h}_i \cdot \mathbf{u}) \quad (19)$$

The solution space of $\delta_i(t)$ and $\Omega_i(t)$ can be achieved when J_H reaching to the maximum value. The maximum angular momentum of the VSCMG can be achieved when substituted the solution space of $\delta_i(t)$ and $\Omega_i(t)$ into the following equation.

$$\mathbf{H} = \sum_{i=1}^4 J\Omega_i(t) \mathbf{s}_i [\delta_i(t)] \quad (20)$$

The maximum angular momentum envelop of the SGCMG is made up of all 4H singular surface and part 2H singular surface. Consequently, the following equation can be achieved when J_H reach to the maximum value.

$$J_H = \mathbf{H} \cdot \mathbf{u} = \sum_{i=1}^4 |\mathbf{h}_i \cdot \mathbf{u}| \quad (21a)$$

$$J_H = \mathbf{H} \cdot \mathbf{u} = \sum_{j=1, j \neq i}^4 |\mathbf{h}_j \cdot \mathbf{u}| - |\mathbf{h}_i \cdot \mathbf{u}| \quad (21b)$$

Equation (21a) means that the sign of $\mathbf{h}_i \cdot \mathbf{u}$ (where $i = 1, 2, 3, 4$) are all positive sign. For the convenience of problem description, this situation can be marked as case 1. Under this situation, $\mathbf{h}_i \cdot \mathbf{u}$ can reach to the maximum value when current gimbals staying at the singular gimbals positions. Equation (21b) means that the sign of $\mathbf{h}_i \cdot \mathbf{u}$ is the minus sign, and the sign of $\mathbf{h}_j \cdot \mathbf{u}$ ($i \neq j$) are positive sign. For the convenience of problem description, this situation can be marked as case 2. Under this situation, $\mathbf{h}_i \cdot \mathbf{u}$ can reach to the maximum value when gimbals staying at singular gimbals positions, meanwhile, $\mathbf{h}_j \cdot \mathbf{u}$ can reach to the minimum value when the gimbals staying at singular gimbals positions.

In the VSCMG system, the following equation can be achieved when J_H reach to the maximum value.

$$J_H = \mathbf{H} \cdot \mathbf{u} = \sum_{i=1}^4 J\Omega_i(t) |\mathbf{s}_i \cdot \mathbf{u}| \quad (22a)$$

$$J_H = \mathbf{H} \cdot \mathbf{u} = \sum_{j=1, j \neq i}^4 J\Omega_j(t) |\mathbf{s}_j \cdot \mathbf{u}| - J\Omega_i(t) |\mathbf{s}_i \cdot \mathbf{u}| \quad (22b)$$

Equation (22a) means that the sign of $\mathbf{s}_i \cdot \mathbf{u}$ (where $i = 1, 2, 3, 4$) are all positive sign (Case 1). Equation (22b) means that the sign of $\mathbf{s}_i \cdot \mathbf{u}$ is the minus sign, and the sign of $\mathbf{s}_j \cdot \mathbf{u}$ ($i \neq j$) are positive sign (Case 2).

The maximum angular momentum surface of the VSCMG with upper and lower bound limitation of the flywheel regulation speed can be expressed as following two cases.

Case 1: J_H can reach to the maximum value when the gimbals staying at singular gimbals positions and the flywheel speed is approaching to the maximum value. Consequently, the maximum angular momentum of the VSCMG can be expressed as follows.

$$\mathbf{H} = \sum_{i=1}^4 \frac{(\mathbf{g}_i \times \mathbf{u}) \times \mathbf{g}_i}{|\mathbf{g}_i \times \mathbf{u}|} J \Omega_{\max} \tag{23}$$

Case 2: under this situation, the maximum angular momentum of the VSCMG can be expressed as following optimization problem.

$$\begin{aligned} \max_{\delta(t), \Omega(t)} \mathfrak{J} &= J \sum_{i=1}^4 \Omega_i \mathbf{s}_i \cdot \mathbf{u}_j^* \\ \text{s.t. } & J \sum_{i=1}^4 \Omega_i \cos \xi_i \mathbf{n}_i = \mathbf{0}_{2 \times 1} \end{aligned} \tag{24}$$

To sum up, the maximum angular momentum envelop of the VSCMG with upper and lower bound limitation of the flywheel regulation speed is the approximate ellipsoid with eight symmetric distribution hollows when $\beta \in (0^\circ, 90^\circ)$. The minimum momentum value can be achieved at the hollow point on the maximum momentum envelop. The value of the maximum angular momentum is directly related to Ω_{\max} and Ω_{\min} .

5) The maximum angular momentum envelop when $\beta = 0^\circ$

Equation (1) can be rewritten as follows when $\beta = 0^\circ$.

$$\mathbf{H} = J \Omega_1 \begin{bmatrix} -s\delta_1 \\ c\delta_1 \\ 0 \end{bmatrix} + J \Omega_2 \begin{bmatrix} -c\delta_2 \\ -s\delta_2 \\ 0 \end{bmatrix} + J \Omega_3 \begin{bmatrix} s\delta_3 \\ -c\delta_3 \\ 0 \end{bmatrix} + J \Omega_4 \begin{bmatrix} c\delta_4 \\ s\delta_4 \\ 0 \end{bmatrix} \tag{25}$$

According to analysis of Equation (25), the angular momentum in xoy plane for the task of attitude control can be covered by the VSCMG when $\beta = 0^\circ$. The Jacobian matrix can be rewritten as follows when $\beta = 0^\circ$.

$$\mathbf{C} = J \begin{bmatrix} -c\delta_1\Omega_1 & s\delta_2\Omega_2 & c\delta_3\Omega_3 & -s\delta_4\Omega_4 \\ -s\delta_1\Omega_1 & -c\delta_2\Omega_2 & s\delta_3\Omega_3 & c\delta_4\Omega_4 \\ 0 & 0 & 0 & 0 \end{bmatrix} \tag{26a}$$

$$\mathbf{D} = J \begin{bmatrix} -s\delta_1 & -c\delta_2 & s\delta_3 & c\delta_4 \\ c\delta_1 & -s\delta_2 & -c\delta_3 & s\delta_4 \\ 0 & 0 & 0 & 0 \end{bmatrix} \tag{26b}$$

According to analysis Equation (26a) and Equation (2b), we can get the follows conclusion that the gyroscopic torque of the four gimbals and the reaction torque of the four flywheels cannot along the direction of z axis. The gyroscopic torque of each unit will approach to the maximum value that is along the x axis or y axis when the reaction torque of each unit approaching to the minimum value. The maximum angular momentum envelop of the VSCMG can be expressed as follows when $\beta = 0^\circ$.

According to analyze **Figure 4**, we can get the conclusion that the angular momentum requirement of the spacecraft in xoy plan can be satisfied by the VSCMG when $\beta = 0^\circ$, unfortunately, the angular momentum requirement of the spacecraft along the z axis cannot be covered by the VSCMG when $\beta = 0^\circ$. Under this situation, the ability of output torque of the flywheel torque will approach to the maximum value along the x axis when $\delta_1 = 90^\circ$, $\delta_2 = 0^\circ$, $\delta_3 = 90^\circ$

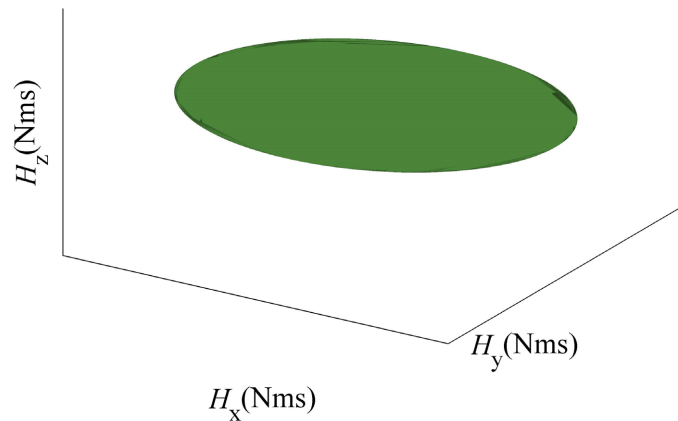


Figure 4. The angular momentum envelop of VSCMG when $\beta = 0^\circ$

and $\delta_4 = 0^\circ$. The ability of output torque of the flywheel torque will approach to the maximum vale along the y axis when $\delta_1 = 0^\circ$, $\delta_2 = 90^\circ$, $\delta_3 = 0^\circ$ and $\delta_4 = 90^\circ$. The following designed idea can be achieved. Consequently, the flywheel torque can be reduced when $\beta = 0^\circ$ and the output torque is along the x axis or y axis.

6) The maximum angular momentum envelop when $\beta = 90^\circ$

Equation (1) can be rewritten as follows when $\beta = 90^\circ$.

$$H = J\Omega_1 \begin{bmatrix} 0 \\ c\delta_1 \\ s\delta_1 \end{bmatrix} + J\Omega_2 \begin{bmatrix} -c\delta_2 \\ 0 \\ s\delta_2 \end{bmatrix} + J\Omega_3 \begin{bmatrix} 0 \\ -c\delta_3 \\ s\delta_3 \end{bmatrix} + J\Omega_4 \begin{bmatrix} c\delta_4 \\ 0 \\ s\delta_4 \end{bmatrix} \quad (27)$$

According to analyze Equation (27), The Jacobian matrix can be rewritten as follows when $\beta = 90^\circ$.

$$C = J \begin{bmatrix} 0 & s\delta_2\Omega_2 & 0 & -s\delta_4\Omega_4 \\ -s\delta_1\Omega_1 & 0 & s\delta_3\Omega_3 & 0 \\ c\delta_1\Omega_1 & c\delta_2\Omega_2 & c\delta_3\Omega_3 & c\delta_4\Omega_4 \end{bmatrix} \quad (28a)$$

$$D = J \begin{bmatrix} 0 & -c\delta_2 & 0 & c\delta_4 \\ c\delta_1 & 0 & -c\delta_3 & 0 \\ s\delta_1 & s\delta_2 & s\delta_3 & s\delta_4 \end{bmatrix} \quad (28b)$$

According to analysis of Equation (28a) and Equation (28b), we can get the following conclusion that the angular momentum of the task of the attitude control with three-dimensional space will be covered by VSCMG when $\beta = 90^\circ$. The three dimensional torque requirement can be satisfied by the VSCMG when $\beta = 90^\circ$.

According to **Figure 5**, we can get the conclusion that the angular momentum requirement of the spacecraft can be satisfied by the VSCMG when $\beta = 0^\circ$. Under this situation, the ability of output torque of the reaction torque can approach to the maximum value and along the z axis when $\delta_1 = 90^\circ$, $\delta_2 = 90^\circ$, $\delta_3 = 90^\circ$ and $\delta_4 = 90^\circ$. The following designed idea can be achieved. Consequently, the flywheel torque can be reduced when $\beta = 90^\circ$ and the output

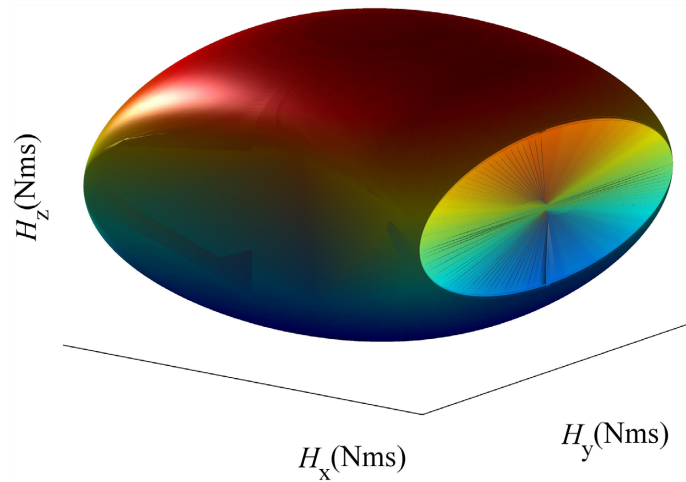


Figure 5. The angular momentum envelop of VSCMG when $\beta = 90^\circ$.

torque is along the z axis.

2. The New Designed Steering Law

In the following section, the steering law is redesigned for the VSCMG with variable skew angle. The singularity can be avoided, and the torque requirement of the flywheel can be reduced.

1) The expected steering results of the gimbals and the flywheels

In the process of the new designed steering, in order to minimizing the system power, the following performance function can be introduced.

$$\min \quad \mathfrak{J}_4 = \frac{1}{2} \begin{bmatrix} \dot{\delta} \\ \dot{\Omega} \end{bmatrix}^T \mathbf{W}_1^{-1} \begin{bmatrix} \dot{\delta} \\ \dot{\Omega} \end{bmatrix} \quad (29)$$

The system power has upper bound limitation of the actual realizable system. Besides, there is no gyroscopic torque with variable gimbals positions when the flywheel speed approaching to zero. Therefore, the flywheel should have upper bound limitation and lower bound limitation. So the bi-directional output torque cannot always be output with regulation flywheel speed. The ability of bi-directional torque will be output with additional ability of flywheel speed equalization. So Equation (29) can be rewritten as follows.

$$\min \quad \mathfrak{J}_4 = \frac{1}{2} \begin{bmatrix} \dot{\delta} \\ \dot{\Omega} \end{bmatrix}^T \mathbf{W}_1^{-1} \begin{bmatrix} \dot{\delta} \\ \dot{\Omega} \end{bmatrix} + \mathbf{R} \begin{bmatrix} \dot{\delta} \\ \dot{\Omega} \end{bmatrix} \quad (30)$$

where \mathbf{W}_1 is the weighted matrix. The gimbals positions can be steered far away from singular gimbals positions with reasonable steering gimbal speed. The singularity avoidance strategy can be designed as follows. The torque requirement for the attitude control can be mainly provided by the gyroscopic torque when the gimbals are far away from singular gimbals positions, the torque requirement of the attitude control can be mainly supported by the reaction torque of the flywheels when the gimbals approaching to the singular gimbals positions. Consequently, \mathbf{W}_1 is directly related to the singularity measurement function. In

additional, each flywheel speed will approach to some certain same speed by the adding item of $\mathbf{R}[\delta^T \dot{\Omega}^T]^T$. In order to steer all flywheel speed to some certain same speed ($\bar{\Omega}$), the specific form of \mathbf{R} can be directly related to the deviation between each flywheel speed and $\bar{\Omega}$. The specific form design process of \mathbf{W}_1 and \mathbf{R} can be deduced as following section.

Based on the theory of Singular Value Decomposition (SVD), \mathbf{C} can be re-written as follows.

$$\mathbf{C} = \mathbf{U}\mathbf{\Lambda}\mathbf{V}^T \tag{31}$$

where $\mathbf{U} = [\mathbf{n}_1 \ \mathbf{n}_2 \ \mathbf{n}_3]$, and $\mathbf{V} = [\mathbf{v}_1 \ \mathbf{v}_2 \ \mathbf{v}_3 \ \mathbf{v}_4]$ are unitary matrix, which satisfy the equations $\mathbf{U}^T\mathbf{U} = \mathbf{I}$ and $\mathbf{V}^T\mathbf{V} = \mathbf{I}$, \mathbf{I} represents the identity matrix, and $\mathbf{\Lambda} = [\mathbf{S} \ \mathbf{0}_{3 \times 1}]$, $\mathbf{S} = \text{diag}(\sigma_1 \ \sigma_2 \ \sigma_3)$, and $\sigma_1 > \sigma_2 > \sigma_3 \geq 0$ are singular value of $\mathbf{\Lambda}$.

The pre-existing definition of singularity measurement function can be shown as following form [11].

$$\kappa = \frac{1}{\kappa} = \frac{\sigma_1}{\sigma_3} \tag{32}$$

The denominators of κ will approach to zero when the gimbals approaching to singular gimbals positions. κ will approach to infinity value. The reduction rank of \mathbf{C} will be appeared. The steering results will deteriorate. In order to avoid such situation, the new singular measurement function can be redefined as follows.

$$\kappa_s = \frac{1}{\kappa} = \frac{\sigma_3}{\sigma_1} \tag{33}$$

Under this situation, the specific form design process of \mathbf{W}_1 and \mathbf{R} can be deduced as follows. \mathbf{W}_1 can be redesigned as

$\mathbf{W}_1 = \text{diag}(e^{\rho\kappa_s} - 1, e^{\rho\kappa_s} - 1, e^{\rho\kappa_s} - 1, e^{\rho\kappa_s} - 1, 1, 1, 1, 1)$, ρ is the design parameter. The flywheel can be steered when the gimbals staying at singular gimbals positions. Under this situation, the additional requirement of flywheel torque will be needed when flywheel speed equilibrium is required. Consequently, the flywheel torque can be increased. The flywheel power can be expressed as product of the flywheel torque and the flywheel speed. Consequently, the flywheel power can be increased. In summary, \mathbf{R} can be redesigned as follows.

$$\mathbf{R} = \begin{bmatrix} \mathbf{0}_{1 \times 4} & (\mathbf{W}_R \zeta)^T \end{bmatrix} \tag{34}$$

where $\mathbf{W}_R = (e^{\rho\kappa_s} - 1)\mathbf{I}_{4 \times 4}$. The function of \mathbf{W}_R can be shown in **Figure 6**.

According to **Figure 6**, the function of flywheel speed equilibrium can be executed by steering flywheels when the gimbals are far away from singular gimbals positions. The function of flywheel speed equilibrium cannot be worked by steering flywheel when the gimbals staying at singular gimbals positions. The function of singularity avoidance and flywheel speed equalization will not be worked at the same time. So the flywheel torque can be reduced.

The flywheel speed of the unit i will be de-accelerated by $\mathbf{R}[\delta^T \dot{\Omega}^T]^T$ when

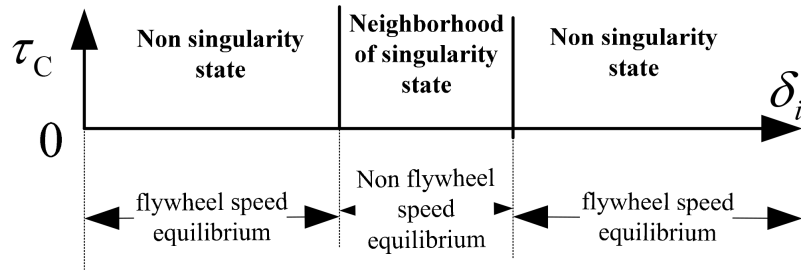


Figure 6. The method of flywheel speed equalization.

$\Omega_i > \bar{\Omega}$. The flywheel speed of the unit i will be accelerated by $R[\delta^T \dot{\Omega}^T]^T$ when $\Omega_i < \bar{\Omega}$. The ability of flywheel speed equilibrium can be achieved, so the flywheel speed of the unit i can approach to $\bar{\Omega}$.

In order to satisfy the torque requirement of the attitude control, it can be provided by gyroscopic torque and reaction torque of the flywheel. The following constraint should be satisfied for the new designed steering law.

$$\tau_c = C\dot{\delta} + D\dot{\Omega} = [C \quad D] \begin{bmatrix} \dot{\delta} \\ \dot{\Omega} \end{bmatrix} \tag{35}$$

where τ_c is the torque requirement of the spacecraft.

The expected steering results can be deduced by combing with Equation (30) and Equation (35). The expected steering results of the new design steering law can be shown as following equation.

$$\begin{bmatrix} \dot{\delta}_d \\ \dot{\Omega}_d \end{bmatrix} = W_1 [Q^T (QW_1 Q^T)^{-1} (\tau_c + QW_1 R^T) - R^T] \tag{36}$$

The function of the flywheel speed equilibrium and the function of the torque for the attitude control can be realized when the expected steering results of the gimbals and the flywheels can be given as Equation (36). In the next following section, the expected steering results of the skew angle are given.

2) The expected steering results of the variable skew angle

The torque of the attitude control can be mainly provided by the flywheels when the gimbals staying at singular gimbals positions. Under this situation, Equation (35) can be rewritten as follows.

$$\tau_c = J \sum_{i=1}^4 s_i \dot{\Omega}_i \tag{37}$$

Based on analysis of the Ref. [5], the vector function of Equation (37) can be rewritten as algebraic equation (gimbals positions are $[-90^\circ, 0^\circ, 90^\circ, 0^\circ]$) and can be expressed as follows.

$$\tau_c \cdot u = J \sum_{i=1}^4 s_i \cdot u \dot{\Omega}_i \tag{38}$$

The requirement of the torque of the flywheel for the task of the attitude control can be deduced as combing with Equation (30) and Equation (38) and can be shown as follows.

$$t_i = \frac{J\dot{\Omega}_i}{\tau_c} = \frac{\pm |\mathbf{g}_i \times \mathbf{u}|}{\sum_{i=1}^4 (\mathbf{g}_i \times \mathbf{u})^2} \tag{39}$$

The following figure can be gotten by calculating of Equation (39) when the output torque is along the x axis.

According to **Figure 7**, we can get the following conclusion that the torque requirement of each flywheel can be increased with variable skew angle. In order to minimize the flywheel torque, the expected steering results of the variable skew angle can be designed as following equation when the output torque is along the x axis or y axis.

$$\boldsymbol{\beta}_d = [0^\circ, 0^\circ, 0^\circ, 0^\circ]^\text{T} \tag{40}$$

The torque requirement of the flywheels for the task of the attitude control can be formed as Equation (39) when the gimbals staying at singular gimbals positions (the gimbals positions are $[90^\circ, 90^\circ, 90^\circ, 90^\circ]$) and the torque is along the z axis. The following figure can be gotten according to calculate of Equation (39) when the output torque is along the z axis.

According to **Figure 8**, we can get the following conclusion that the torque requirement of the flywheels can be decreased with decreasing skew angle. Base on above analysis results, the expected steering results of skew angle can be shown as follows when the output torque is along the z axis.

$$\boldsymbol{\beta}_d = [90^\circ, 90^\circ, 90^\circ, 90^\circ]^\text{T} \tag{41}$$

In order to steer the current skew angle to $\boldsymbol{\beta}_d$, the performance function can

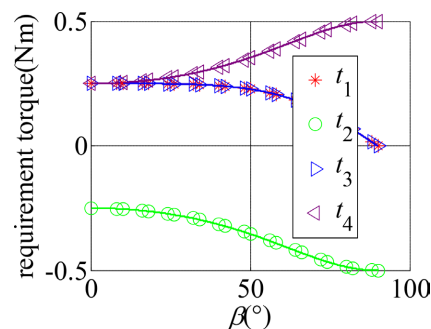


Figure 7. The requirement torque of the flywheels.

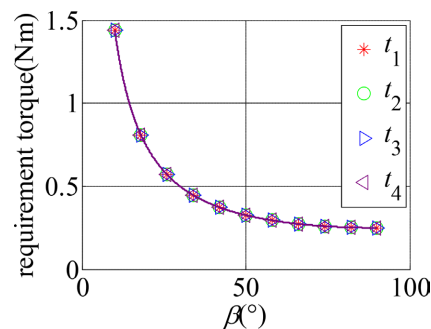


Figure 8. The requirement torque of the flywheels.

be redefined as follows.

$$\mathfrak{J} = k\beta_e^T \beta_e = k(\beta - \beta_d)^T (\beta - \beta_d) \tag{42}$$

The performance function can be deduced as following form.

$$\frac{d\mathfrak{J}}{dt} = \nabla \mathfrak{J} \dot{\beta} = k_{\beta} \sum_{i=1}^4 (\beta_i - \beta_{di}) \tag{43}$$

where $k_{\beta} > 0$ is a design parameter.

According to above analysis, we can get the span of the skew angle can be shown as $\beta \in [0^{\circ}, 90^{\circ}]$.

3) The redesigned steering law

In order to follow the expected steering results, the new performance function of the new designed steering law should be redesigned as following form.

$$L = \min \frac{1}{2} [\mathbf{v}_e^T \mathbf{A} \mathbf{v}_e + \mathbf{T}_e^T \mathbf{B} \mathbf{T}_e] \tag{44}$$

where $\mathbf{v}_e = \mathbf{v} - \mathbf{v}_d$, $\mathbf{v} = [\dot{\delta} \ \dot{\Omega} \ \dot{\beta}]^T$, $\mathbf{v}_d = [\dot{\delta}_d \ \dot{\Omega}_d \ \dot{\beta}_d]^T$, $\mathbf{A} = \mathbf{I}_{12 \times 12}$. $\mathbf{T}_e = [\mathbf{C} \ \mathbf{D} \ \mathbf{E}] [\dot{\delta} \ \dot{\Omega} \ \dot{\beta}]^T - \tau_c$ is the torque deviation between the torque requirement of attitude control and output torque of the VSCMG with variable skew angle of the pyramid configuration. $\mathbf{B} = \vartheta \mathbf{I}_{3 \times 3}$. ϑ is a design parameter. We can make sure that the second derivative of the performance function L greater than zero when we set $\vartheta > 0$. So L has the minimum value.

The new designed steering law can be deduced based on the first derivative of the performance function L when we setting it to zero. The new designed steering law can be expressed as follows.

$$\mathbf{v} = (\mathbf{A} + \mathbf{W}_n^T \mathbf{B} \mathbf{W}_n)^{-1} (\mathbf{A} \mathbf{v}_d + \mathbf{W}_n^T \mathbf{B} \tau_c) \tag{45}$$

According to Equation (45), we can get the conclusion that $\mathbf{v} \rightarrow \mathbf{v}_d$ when $\partial L / \partial \mathbf{v} = \mathbf{0}_{12 \times 1}$. So \mathbf{v} will approach to \mathbf{v}_d when we set $\vartheta > 0$, So we can get $\dot{\delta} \rightarrow \dot{\delta}_d$, $\dot{\Omega} \rightarrow \dot{\Omega}_d$, $\dot{\beta} \rightarrow \dot{\beta}_d$.

3. The Constant Analysis of Singularity Avoidance

The SGCMG singularly avoidance characteristics of the new designed steering law can be expressed as the maximum torque requirement of the gyroscopic torque and the reaction torque. In this section, the maximum torque requirement of the gyroscopic torque and the reaction torque will be deduced in the following section.

1) The maximum torque requirement of the gyroscopic torque

The maximum gyroscopic torque for attitude control will be appeared when the attitude control is provided by the minimum number of the gimbals. The minimum number of gimbals can be given by the following analysis results. In order to achieve the maximum gyroscopic torque of the gimbals, such situation will be analyzed in the flowing process.

The characteristics of the output torque with different number can be analyzed. According to Equation (8), for one unit of SGCMG, the direction of gy-

roscopic torque is perpendicular to the direction of the angular momentum, at the same time, the direction of gyroscopic torque is perpendicular to the direction of the gimbal axis. The direction of the gyroscopic torque will be varied with the changeable gimbal position. One unit of SGCMG cannot be controlled for attitude control. So the minimize unit is two with controllable for attitude control. Consequently, the gyroscopic torque will approach to the maximum value when the steerable unit is two. This steering situation can be given as follows: The initial gimbals positions are set as $[0^\circ, 0^\circ, 0^\circ, 0^\circ]$, the direction of the attitude control is along the x axis or y axis.

When we set $\Delta\xi \in (0^\circ, 90^\circ)$. The gyroscopic torque and the reaction torque will be alternated between the gimbals and the flywheels when the gimbals positions are $[-90^\circ + \Delta\xi, 0^\circ, 90^\circ - \Delta\xi, 0^\circ]$. The gyroscopic torque will be output when the gimbals positions between $[0^\circ, 0^\circ, 0^\circ, 0^\circ]$ and $[-90^\circ + \Delta\xi, 0^\circ, 90^\circ - \Delta\xi, 0^\circ]$. The flywheel torque will be output when the gimbals positions between $[-90^\circ + \Delta\xi, 0^\circ, 90^\circ - \Delta\xi, 0^\circ]$ and $[-90^\circ, 0^\circ, 90^\circ, 0^\circ]$. The following constraints can be achieved when the gimbal position between $[0^\circ, 0^\circ, 0^\circ, 0^\circ]$ and $[-90^\circ + \Delta\xi, 0^\circ, 90^\circ - \Delta\xi, 0^\circ]$, at the same time, the output torque is along the x axis.

$$\sum_{i=1}^4 \mathbf{n}_{ci} \cos \omega_{ci} J \Omega_i \dot{\delta}_{i\Gamma} + \sum_{i=1}^4 \mathbf{n}_{si} \cos \omega_{si} J \dot{\Omega}_{i\Gamma} = \mathbf{0}_{3 \times 1} \tag{46a}$$

$$Jc\beta \cos \Delta\xi (-\Omega_1 \dot{\delta}_1 + \Omega_3 \dot{\delta}_3) = |\boldsymbol{\tau}_C| \tag{46b}$$

where \mathbf{n}_{ci} and \mathbf{n}_{si} is the projection in the plane Γ_Ω of \mathbf{c}_i and \mathbf{s}_p respectively. $\boldsymbol{\tau}_C$ is vertical vector to the plane of Γ_Ω . ω_{ci} is the angular between \mathbf{n}_{ci} and \mathbf{c}_i . ω_{si} is the angular between \mathbf{n}_{si} and \mathbf{s}_p . According to above analysis results, The maximum gyroscopic torque will be appeared when the flywheel speed is set as Ω_{\min} . Under this situation, Equation (46b) can be rewritten as following equation with consideration of the minimizing gimbal power.

$$J \Omega_{\min} \dot{\delta}_{\max} = \frac{1}{2c\beta \cos \Delta\xi} |\boldsymbol{\tau}_C| \tag{47}$$

where $\dot{\delta}_{\max}$ is the maximum gimbal speed. The maximum gimbal acceleration can be appeared when Equation (47) is satisfied. The maximum gimbal acceleration can be achieved and expressed as following equation by the first order differential $\dot{\delta}_{\max}$ in Equation (47).

$$\ddot{\delta}_{\max} = \frac{|\boldsymbol{\tau}_C|}{2} \frac{1}{J \Omega_{\min} c\beta} \frac{\sin \Delta\xi}{\cos^2 \Delta\xi} \max \left(\frac{d\Delta\xi}{dt} \right) \tag{48}$$

where $\max(d\Delta\xi/dt) = \dot{\delta}_{\max}$.

2) The maximum torque requirement of reaction torque of the flywheels.

The torque requirement of the attitude control can be provided by the flywheel torque when the gimbals positions between $[-90^\circ + \Delta\xi, 0^\circ, 90^\circ - \Delta\xi, 0^\circ]$ and $[-90^\circ, 0^\circ, 90^\circ, 0^\circ]$. So the following constraints can be satisfied when the output torque is along the x axis.

$$\sum_{i=1}^4 \mathbf{n}_{ci} \cos \omega_{ci} J \Omega_i \dot{\delta}_{i\Gamma} + \sum_{i=1}^4 \mathbf{n}_{si} \cos \omega_{si} J \dot{\Omega}_{i\Gamma} = \mathbf{0}_{3 \times 1} \tag{49a}$$

$$J\dot{\Omega}_1 \mathbf{s}_1 \cdot \boldsymbol{\tau}_C + 2J\dot{\Omega}_m c\beta \sin \Delta\xi + J\dot{\Omega}_3 \mathbf{s}_3 \cdot \boldsymbol{\tau}_C = \boldsymbol{\tau}_C \cdot \boldsymbol{\tau}_C \tag{49b}$$

where $m = 2, 4$.

The torque requirement of the flywheel can be achieved by solving Equation (49b) with minimizing flywheel power. The flywheel torque can be expressed as follows.

$$\frac{J\dot{\Omega}_{\max}}{|\boldsymbol{\tau}_C|} = \max \left(\max_{\beta, \Delta\xi} \frac{\alpha_n}{\alpha_1^2 + \alpha_3^2 + 2c^2 \beta \sin^2 \Delta\xi}, \max_{\beta, \Delta\xi} \frac{c\beta \sin \Delta\xi}{\alpha_1^2 + \alpha_3^2 + 2c^2 \beta \sin^2 \Delta\xi} \right) \tag{50}$$

where $\dot{\Omega}_{\max}$ is the maximum flywheel acceleration, $n = 1, 3$. $\alpha_1 = \mathbf{s}_1 \cdot \boldsymbol{\tau}_C$, $\alpha_3 = \mathbf{s}_3 \cdot \boldsymbol{\tau}_C$. Based on Equation (15), We can get $c\beta \sin \Delta\xi \leq \alpha_n$, so Equation (50) can be rewritten as follows.

$$\frac{J\dot{\Omega}_{\max}}{|\boldsymbol{\tau}_C|} = \max_{\beta, \Delta\xi} \frac{\alpha_m}{\alpha_1^2 + \alpha_3^2 + 2c^2 \beta \sin^2 \Delta\xi} \tag{51}$$

According to analyze of Equation (51), the flywheel torque will be increased with increasing distance that the gimbals are far away from the singular gimbals positions.

3) The avoidance of saturation singularity

The attitude control task cannot be successful implemented when the saturation singularity is encountered. The saturation singularity cannot be effectively avoided by any steering law. If the maximum requirement of the angular momentum for the task of the attitude is wrapped up by the maximum exchangeable angular momentum envelop of the VSCMG, the saturation singularity cannot be encountered during the process of the attitude control task. The whole angular momentum can be exchanged between the spacecraft and the VSCMG. So the maximum requirement of the angular momentum for the task of the attitude (\mathbf{H}_M) is wrapped up by maximum angular momentum envelop of the VSCMG, the saturation singularity cannot encountered during the whole process of the attitude control task. So we can get the following equation.

$$\mathbf{H}_M \leq \mathbf{H}_E \tag{52}$$

where \mathbf{H}_E is the exchangeable angular momentum of the VSCMG with variable skew angular. If Equation (52) is satisfied, the saturation singularity can be effectively avoided. \mathbf{H}_E can be expressed as the radius of the inscribed circle by calculating of the following equation.

$$\mathbf{H} = \sum_{j=1, j \neq i}^4 \frac{(\mathbf{g}_j \times \mathbf{u}) \times \mathbf{g}_j}{|\mathbf{g}_j \times \mathbf{u}|} J\Omega_{\max} - \frac{(\mathbf{g}_i \times \mathbf{u}) \times \mathbf{g}_i}{|\mathbf{g}_i \times \mathbf{u}|} J\Omega_{\min} \tag{53}$$

If we set $S_C = (\Omega_{\max} - \Omega_{\min}) / \Omega_{\max}$, we can get $S_C = 0$ when $\Omega_{\max} = \Omega_{\min}$. $S_C = 1$ when $\Omega_{\min} = 0$. \mathbf{H}_E can be further expressed as the radius of the inscribed circle by calculating of the following equation.

$$R_C = \min \left\{ |\mathbf{H}_{OE}|, 4s\beta J\Omega_{\max}, (2 + 2c\beta) J\Omega_{\max} \right\} \tag{54}$$

where R_C is the radius of the inscribed circle. $(2 + 2c\beta) J\Omega_{\max}$ and $4s\beta J\Omega_{\max}$ are the exchangeable angular momentum along the x axis (or y axis) and z axis,

respectively. The relationship between R_C and variable skew angle with different value of S_C can be expressed as following figures when we set $J\Omega_{\max} = 1 \text{ Nms}$, and $\Omega_{\min} = \Omega_{\max} - S_C\Omega_{\max}$.

In **Figure 9(a)**, R_C can reach to the maximum value when $\beta \in (50^\circ, 60^\circ)$. The value of R_C will be increased with increasing the value of the β . The ratio between maximum value of R_C and the angular momentum of the SGCMG with fixing flywheel speed will reach to 111.25%. The exchangeable angular momentum can be increased with the value of S_C .

According to above analysis results, the following constraint should be satisfied for the VSCMG with variable skew angle.

$$|\mathbf{H}_M| \leq R_C \tag{55}$$

If the above constraint is satisfied, the angular momentum requirement of the attitude control can be satisfied. But the conservatism will become great. Consequently, the power and the mass of the whole system will be increased. To reduce conservatism, the constraint of the angular momentum between the actuator and the spacecraft can be rewritten as following equation.

$$H_M \leq \min [2J\Omega_{\max} (1 + c \beta), 4s\beta J\Omega_{\max}] \tag{56}$$

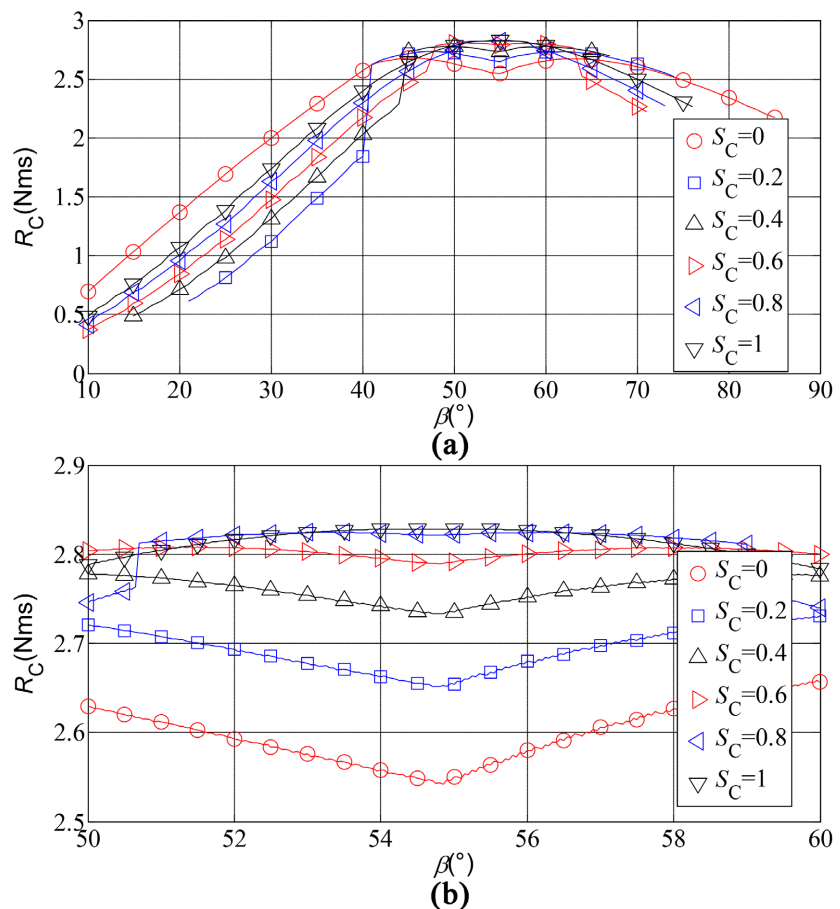


Figure 9. The relationship between R_C and β with different value of S_C . (a) $\beta \in (0^\circ, 90^\circ)$; (b) $\beta \in (50^\circ, 60^\circ)$.

In Equation (56), the exchangeable angular momentum of the VSCMG with variable skew angel along the z axis will approach to zero when $\beta = 0^\circ$. Under this situation, if the disturbance that is along the z axis cannot be damped by the actuator, the ability of attitude control task with three-dimensional cannot be satisfied. The relationship between $(2 + 2c\beta)$ and $4s\beta J$ can be shown as the following figure.

In **Figure 10**, the maximum exchangeable angular momentum of the VSCMG with variable skew angle will approach to 4 with reasonable skew angle regulation. The constraint of the angular momentum between the actuator and the spacecraft can be rewritten as following equation.

$$H_M \leq 2J\Omega_{\max} (1 + \cos \Delta\xi) \tag{57}$$

Under this situation, the minimum exchangeable angular momentum of the VSCMG with variable skew angle for z axis damping (H_D) can be satisfied when $\delta_1 = 0^\circ$, $\delta_2 = 0^\circ$, $\delta_3 = 0^\circ$ and $\delta_4 = 0^\circ$.

$$\min H_D = 4J \sin \Delta\xi \Omega_{\min} \tag{58}$$

If Equation (57) is satisfied, the saturation singularity will not be encountered during the whole process of the task of the attitude control. In another words, the saturation singularity can be effectively avoided.

4) The initial skew angle

If the singularity that is near the zero point of the angular momentum is encountered, the flywheel can be steered by the new designed steering law. There is no enough time to regulate skew angle to appropriate position for minimizing flywheel power. This situation suggests that the power of the skew angle can be increased, which is not suitable for actual system implementation.

According to the Ref. [5], if the constraint steering law is applied. The exchangeable angular momentum are the same along the three axis when $\beta = 26.37^\circ$.

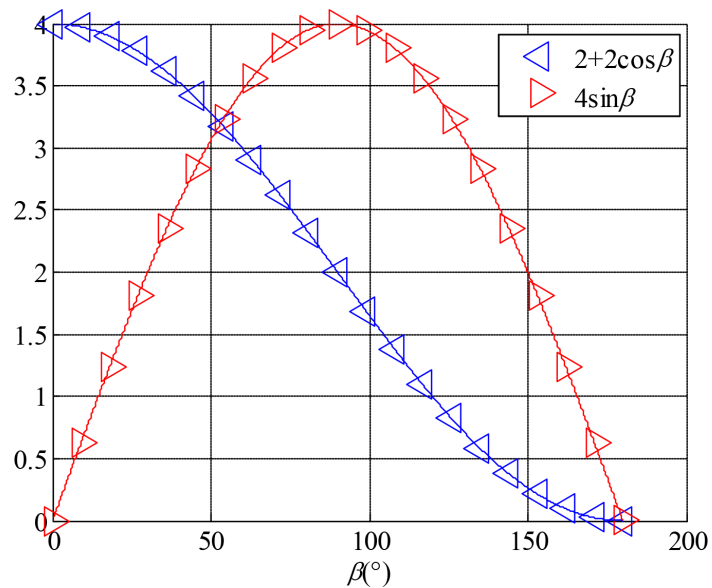


Figure 10. The relationship between $2 + 2c\beta$ and $4s\beta J$ with different value of S_C .

Consequently, the initial skew angle can be set as 26.37° , the maximum skew angle speed can be shown as follows.

$$\begin{aligned} \dot{\beta}_{\max} &= \max\left(\frac{26.37 - \Delta\delta}{t_{\min}}, \frac{90 - \Delta\delta - 26.37}{t_{\min}}\right) \\ t_{\min} &= \frac{2[1 + \cos(26.37)]J\Omega_{\min}}{\|\tau_c\|_2} \end{aligned} \tag{59}$$

The additional flywheel power can be reduced when the initial skew angle is setting as 26.37° .

4. The Optimizing Parameters of the VSCMG for Attitude Control

The problem of the optimizing parameters of the VSCMG with variable skew angle for attitude control can be expressed as follows. The parameters optimizing problem of VSCMG with variable skew angle can be given as follows. The design parameters of the VSCMG with variable skew angle can be given with minimizing whole system power and satisfying the requirement of the attitude control. In order to satisfy the requirement of the attitude control, the angular momentum of the attitude control can be wrapped up by the exchangeable angular momentum of the VSCMG with skew angle (related parameters can be expressed as Ω_{\max} , Ω_{\min} and J). At the same time, the torque requirement of the attitude control can be satisfied by the gyroscopic torque and flywheel torque (related parameters can be expressed as $\dot{\Omega}_{\max}$, $\dot{\delta}_{\max}$ and $\ddot{\delta}_{\max}$) under considering of the singularity avoidance (related parameters can be expressed as $\Delta\xi$, $\dot{\beta}_{\max}$).

The optimizing parameters of the VSCMG for attitude control can be cast as following multi-objective optimizing problem when the angular momentum requirement of the attitude control (H_M) and the torque requirement of the attitude control (τ_c) are known.

$$\begin{aligned} &\min_{J, \Omega_{\min}, \Omega_{\max}, \Delta\xi} P_R + P_G \\ &\max_{J, \Omega_{\min}, \Omega_{\max}, \Delta\xi} S_C = \frac{\Omega_{\max} - \Omega_{\min}}{\Omega_{\max}} \\ &\text{s.t. } H_M \leq 2J\Omega_{\max} (1 + \cos \Delta\xi) \end{aligned} \tag{60}$$

where $f(J, \Omega_{\min}, \Omega_{\max}, \Delta\xi)$ is the objective function with vector form of the parameters optimizing of the VSCMG. P_G is the maximum gimbal power, P_R is the maximum flywheel power. P_G and P_R can be described as follows, respectively.

$$\begin{cases} P_G = J_G \dot{\delta}_{\max} \ddot{\delta}_{\max} = J_G \left(\frac{|\tau_c|}{2J\Omega_{\min} \cos \Delta\xi} \right)^2 \frac{\sin \Delta\xi}{\cos \Delta\xi} \max\left(\frac{d\Delta\xi}{dt}\right) \\ P_R = J\dot{\Omega}_{\max} \Omega_{\max} = \frac{\alpha_m}{\alpha_1^2 + \alpha_3^2 + 2\sin^2 \Delta\xi} |\tau_c| \Omega_{\max} \end{cases} \tag{61}$$

where J_G is the moment of inertia along the direction of the gimbal axis. We can get $J_G \approx J$ when the flywheel momentum of inertia of the gyroscopic room is

considered.

In Equation (61), the maximum flywheel torque can be reduced to the 25% that is the ratio between the torque requirement of the flywheel and the torque requirement of the attitude control when the current gimbals staying at singular gimbals positions. Under this situation, the power requirement of the gimbals will approach to infinity value when the gimbals staying at singular gimbals positions. The characteristics of the contradiction of the multi-objectives optimizing problem can be achieved according to above analysis results. Consequently, the distance ($\Delta\zeta$) that is between the current gimbal position and the singular gimbal position need to be introduced.

The multi-objective optimization problem that can be indicated as Equation (60), that can be solved by the intelligent algorithm of the particle swarm optimization. When we set the $|H_M| = 0.9$ Nms. Meanwhile, the maximum torque for attitude control can be expressed as $|\tau_c| = 0.09$ Nm. The optimization results of the VSCMG with variable skew angle can be expressed as **Table 1**.

According to **Table 1**, the optimization VSCMG with variable skew angle is given. The performance of the attitude control need to be further analyzed. Furthermore, the effectiveness of the singularity avoidance should be further verified. Besides, it is need to be further analyzed the flywheel power and the flywheel torque. All the analysis results will be given in the next following section.

5. Simulation and Verification

In this section, the control system of the whole spacecraft system is built, and the matrix of the inertia of the spacecraft can be set as $I = \text{diag}([10, 10, 10])$. Furthermore, the typical linear controller is applied. Consequently, the influence factors can be effectively reduced, and the ability of singularity avoidance can be clearly verified by the analysis results. Besides, the main problem for the new designed steering law and the optimization VSCMG that is given in the above analysis results is the singularity problem. In summary, the ability of singularity avoidance would be the main problem that should be considered in the section, and the actual steering results of the new designed steering law of the optimization VSCMG with variable skew angle are given in this section.

1) The maneuvering task along the x axis

According to the characteristics of the pyramid configuration, the steering results when the maneuvering task along the x axis and the steering results when

Table 1. The optimization results of the VSCMG.

Parameter	result	Parameter	result
$J(\text{kg}\cdot\text{m}^2)$	9.04×10^{-4}	$(d\Omega/dt)_{\max} (\text{rad/s}^2)$	30
		$(d^2\delta/dt^2)_{\max} (\text{rad/s}^2)$	2.70
$\Omega_{\max} (\text{rpm})$	6377	$(d\delta/dt)_{\max} (\text{rad/s})$	2.20
$\Omega_{\min} (\text{rpm})$	3020	$\Delta\zeta(^{\circ})$	80.05

the maneuvering task along the y axis have the same results. Consequently, the actually steering results along the x axis are analyzed in the following section. The attitude control task can be planned as follows: 24 degree along the x axis in 20 s. Under this situation, in order to verify the ability of the singularity avoidance, the extreme case should be verified in the following section. Consequently, the initial gimbal positions can be set as $[0^\circ, 0^\circ, 0^\circ, 0^\circ]$. According to Ref. [2] and Ref. [5], the minimum steerable number of the gimbals is 2, and the gimbals will be steered approach to the singular gimbal positions. The inescapable singularity will be encountered during the steering process when the output torque is along the x axis (The singular gimbal positions are $[90^\circ, 0^\circ, -90^\circ, 0^\circ]$). The simulator results of the actually steering results of the optimization VSCMG with variable skew angle can be shown as following figures.

In **Figure 11**, φ , θ and ψ are the Euler angles in the inertial coordinate system. The task of the attitude control is planned at above section (large angle maneuvering along the x axis) can be successively operated by the optimization VSCMG with the variable skew angle. The torque that is needed by the task of the attitude control can be mainly provided by the gyroscopic torque when $t < 9.1$ s. The torque for the task of the attitude control will be switched from gyroscopic torque of the gimbals to reaction torque of the flywheels by the new designed steering law when $t = 9.1$ s. The torque of the task of the attitude control that is needed can be mainly provided by reaction torque of the flywheels when $9.1 < t < 10$ s. The flywheel speed deviation will be appeared. The gimbal position of the unit 1 will be steered form 0° to 90° when $t < 9.1$ s. At the same time, the gimbal position of the unit 3 will be steered form 0° to -90° when $t < 9.1$ s. Consequently, the inescapable singularity can be encountered when $t = 9.1$ s (The singular gimbal position are $[90^\circ, 0^\circ, -90^\circ, 0^\circ]$). According to analyze of reaction torque of the flywheels, the output torque of the task of the attitude control will be supported by reaction torque of the flywheels when the singularity is encountered. Consequently, the singularity can be effectively overcome by the variable flywheel speed. The skew angle will be steered towards to the 0 degree when $0 < t < 9.1$. In the system of the VSCMG with variable skew angle, the precisely torque can be output even with rate fluctuations of the skew angle. Consequently, the difficult of the system implement and the cost of the system can be reduced. Under this situation, the value of $s_i \cdot u(i=1,2,3,4)$ will approaching to 1. In order to further verify the effectiveness of the variable skew angle in the VSCMG, the following comparison analysis results are given.

In **Figure 12**, compare with the fixing skew angle and the variable skew angle, the flywheel acceleration and the flywheel power are given with different simulation conditions. According to analysis results, the ability of output torque of the flywheels will be increased when the reasonable skew angle is steered. Consequently, the torque requirement of the flywheels will be decreased, and the flywheel power that is determined by the flywheel torque and the flywheel speed will be reduced.

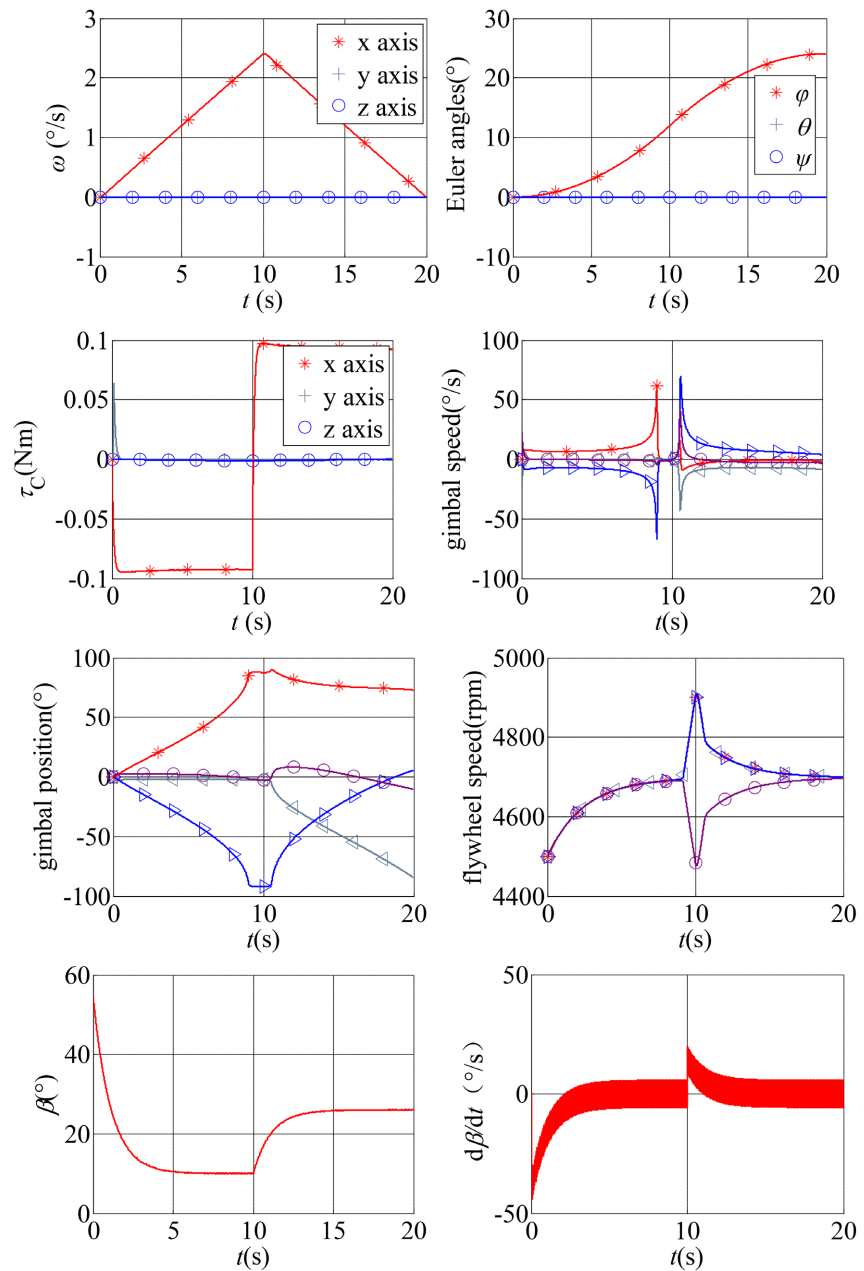


Figure 11. The system response waveform for the optimization VSCMG with variable skew angle (along x axis).

2) The maneuvering task along the z axis

The attitude control task can be planned as follows: 40 degree along the z axis in 20s. In order to verify the ability of the singularity avoidance, the extreme case will be verified in the following section. Consequently, the initial gimbals positions can be set as $[0^\circ, 0^\circ, 0^\circ, 0^\circ]$. Under this situation, all gimbals will be steered from 0° to -90° . Consequently, the singularity will be encountered soon or later for the VSCMG with fixing skew angle (The singular gimbals positions are $[-90^\circ, -90^\circ, -90^\circ, -90^\circ]$). According to **Figure 4** and **Figure 5**, the exchangeable angular momentum envelop along the z axis will be increased for the VSCMG

with variable skew angle when the skew angle is steered from current value to -90° . Based on **Figure 4** and **Figure 5**, the singular gimbal positions (The singular gimbal positions are $[-90^\circ, -90^\circ, -90^\circ, -90^\circ]$) will be delayed by the reasonable steering results of the variable skew angle. The actually steering results can be shown as follows.

According to **Figure 13**, the attitude of the spacecraft will be maneuvered from 0° to 40° in the 20 s. The maximum maneuvering speed can reach to $4^\circ/\text{s}$. Consequently, the attitude maneuvering task can be successfully operated in the fixed time. The singularity cannot be encountered during the maneuvering process. The steering results of the gimbals and the flywheels can be shown in the following section.

In **Figure 14**, the initial gimbal positions are $[0^\circ, 0^\circ, 0^\circ, 0^\circ]$. For the VSCMG with variable skew angle, the minimizing gimbal positions are $[-60^\circ, -60^\circ,$

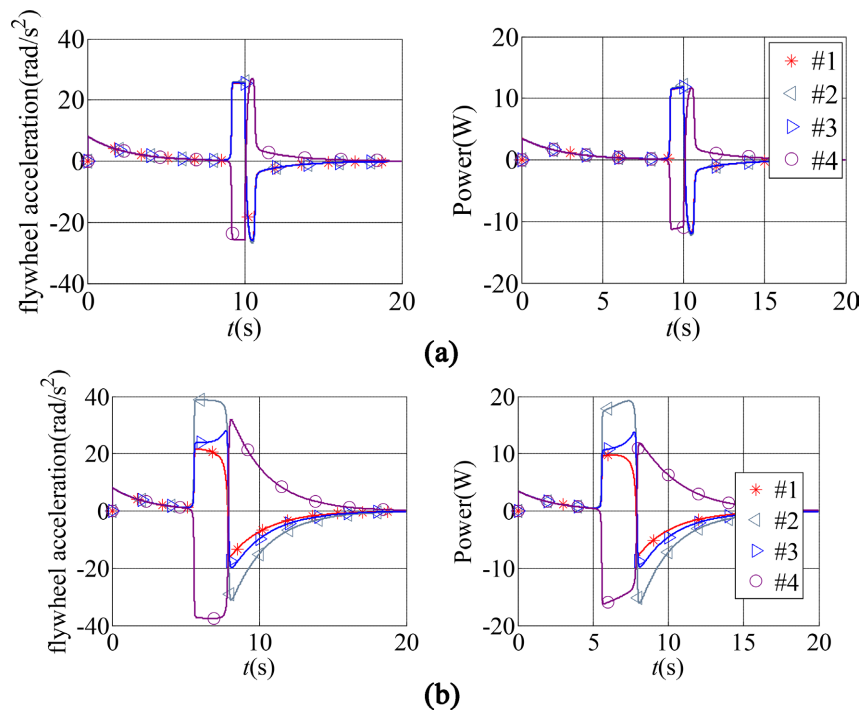


Figure 12. The comparison analysis results of the flywheel torque and flywheel power. (a) Variable skew angle; (b) fixed skew angle ($\beta = 54.74^\circ$).

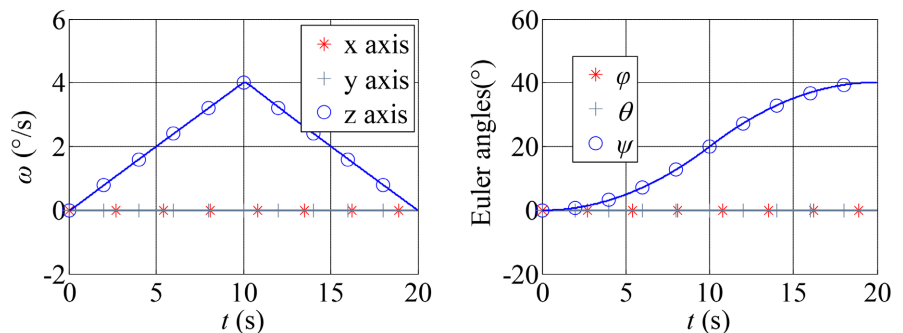


Figure 13. The attitude maneuvering along the z axis.

$-60^\circ, -60^\circ]$ when $t = 10$ s. The singularity can be effectively avoided by the VSCMG with variable skew angle. In another words, the singularity (The singular gimbal positions are $[-90^\circ, -90^\circ, -90^\circ, -90^\circ]$) will be delayed by the VSCMG with variable skew angle. For the VSCMG with fixing skew angel, the minimizing gimbal positions are $[-90^\circ, -90^\circ, -90^\circ, -90^\circ]$ when $t = 9.5$ s. The inescapable singularity will be encountered. Under this situation, the output torque of the VSCMG cannot be supported by the gyroscopic torque of the gimbals, at the same time, the output torque of the VSCMG can be supported by the reaction torque of the flywheels.

According to analyze **Figure 14** and **Figure 15**, the inescapable singularity will be delayed by the VSCMG with variable skew angle. In another words, the inescapable singularity can be effectively avoided by the VSCMG with variable skew with reasonable designing of the steering law. The analysis results are consisted with the theory analysis results that are given in **Figure 4** and **Figure 5**.

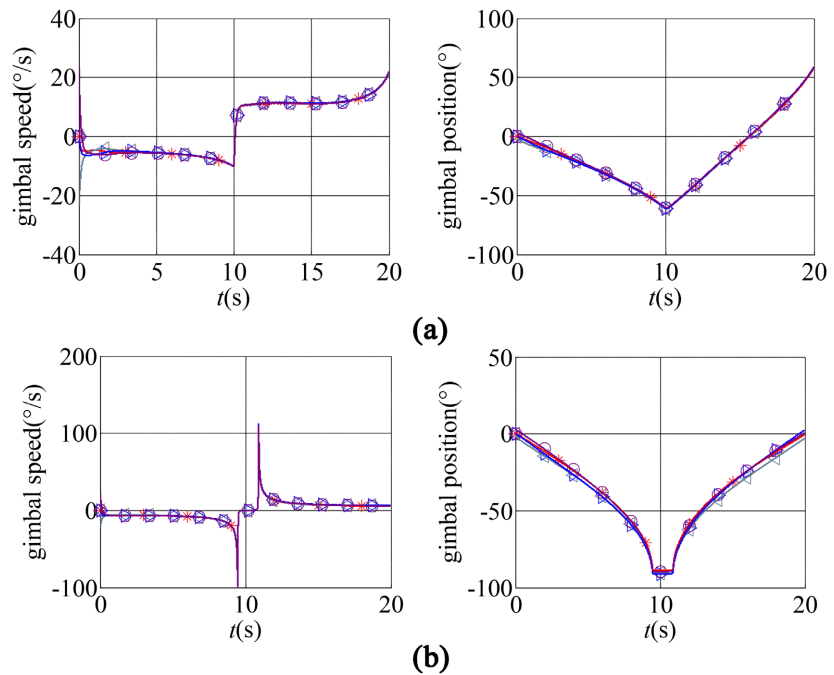


Figure 14. The steering results of the gimbals. (a) Variable skew angle; (b) fixed skew angle ($\beta = 54.74^\circ$).

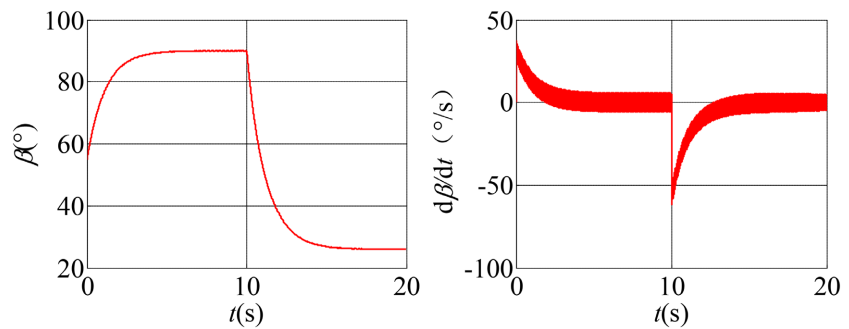


Figure 15. The steering results of the variable skew angle.

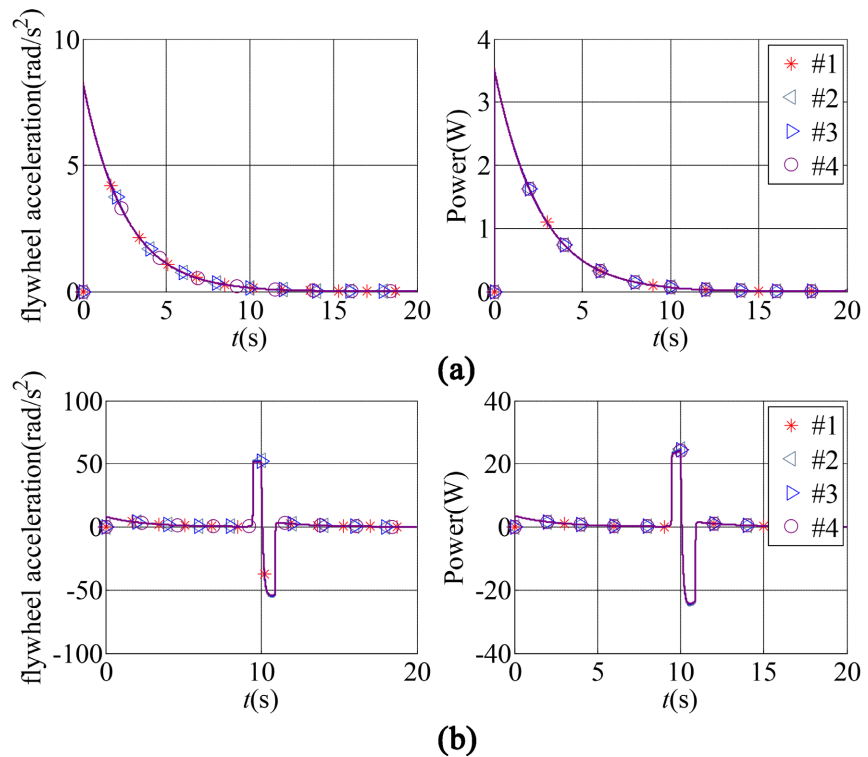


Figure 16. The comparison and analysis of the flywheel power and the flywheel torque. (a) Variable skew angle; (b) fixed skew angle ($\beta = 54.74^\circ$).

In **Figure 16**, some certain reaction torque will be needed at the beginning of the attitude maneuvering task. The reason will be given in the follows. At the beginning of the attitude maneuvering task, the gimbals positions are $[0^\circ, 0^\circ, 0^\circ, 0^\circ]$. The three dimensional torque can be supported by the gyroscopic torque of the gimbals. Unfortunately, under this situation, we can get $\kappa_s \rightarrow 0$. Consequently, the ability of the output torque of the gyroscopic torque will be reduced. In order to satisfy the torque requirement of the attitude control, some certain reaction torque will be needed by \mathcal{W}_1 . For the VSCMG with the fixing skew angle, the inescapable singularity will be encountered when $t = 9.5$ s. Consequently, the output torque for the task of the attitude control will be supported by the reaction torque of the flywheels when the inescapable singularity is encountered. The flywheel torque will be increased. At the same time, the flywheel power that is determined by the flywheel torque and the flywheel speed will be increased. In summary, compare with the VSCMG with fixing skew angle, the flywheel torque and the flywheel power will be decreased with reasonable steering skew angle. The steering results of the flywheel speed can be shown as following figures.

In **Figure 17**, the inescapable singularity will be encountered for the VSCMG with fixing skew angle. Consequently, the additional flywheel torque will be needed for the task of the attitude control. The flywheel speed will be sharply increased. However, the ability of the flywheel speed equalization can be achieved by the new designed steering law.

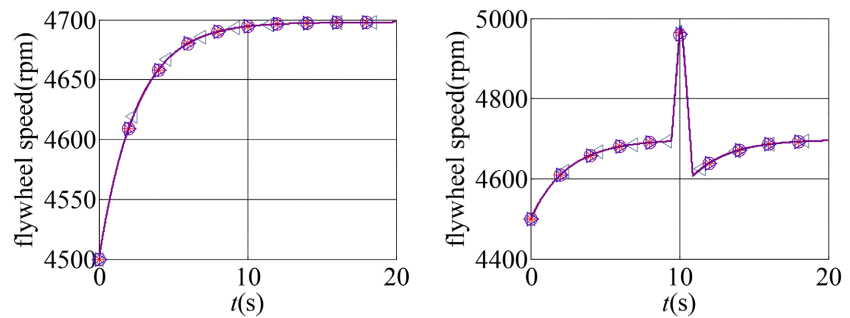


Figure 17. The Comparison analysis of the flywheel speed. (a) Variable skew angle; (b) Fixed skew angle ($\beta = 54.74^\circ$).

6. Conclusion

In this paper, a new strategy of minimizing the flywheel power of the VSCMG with variable skew angle is considered. The exchangeable angle momentum envelop of the VSCMG with variable skew angle is analyzed. Then a new steering law is redesigned for the VSCMG with the variable skew angle. The skew angle can be reasonably steered by the new designed steering law. Consequently, the torque of the attitude control can be mainly provided by the gyroscopic torque at vast majority of the time. The task of the attitude control can be mainly provided by the reaction torque when the singularity is encountered. The skew angle will be reasonably steered by the new designed steering law for the minimizing flywheel torque when the gimbals staying at singular gimbal positions. Consequently, the singularity can be effectively avoided by assisting of the variable skew angle. Later, the optimizing problem of the VSCMG with variable skew angle can be cast as a multi-objective static function with minimizing system power and the maximizing exchangeable angular momentum under consideration about the new designed steering law. The multi-objective static function will be solved by the intelligent algorithm of the particle swarm optimization. Although, the utilization ratio of the angular momentum is decreased, the flywheel power can be decreased. The inescapable singularity can be avoided, and the whole system power can be decreased.

Acknowledgements

This research work is supported by the Natural Science Foundation of Ningxia Province (Grant No. 2021AAC03171). This research work is also supported by the National Natural Science Foundation of China (Grant No. 62163003).

Conflicts of Interest

The authors declare no conflicts of interest regarding the publication of this paper.

References

- [1] Liu, F., Zhao, H., Yao, Y., *et al.* (2016) The Parameters Optimisation Design for Va-

- riable Speed Control Momentum Gyroscopes. *International Journal of Control*, **90**, 2618-2630. <https://doi.org/10.1080/00207179.2016.1261304>
- [2] Liang, T. and Xu, S.J. (2005) Geometric Analysis of Singularity for Single-Gimbal Control Moment Gyro Systems. *Chinese Journal of Aeronautics*, **18**, 295-303. [https://doi.org/10.1016/S1000-9361\(11\)60248-3](https://doi.org/10.1016/S1000-9361(11)60248-3)
- [3] Lappas, V.J. (2002) A Control Moment Gyro (CMG) Based Attitude Control System (ACS) for Agile Small Satellites. Master's Thesis, University of Surrey, Guildford.
- [4] Liu, F., Gao, F., Zhang, W.W., Zhang, B. and He, J.H. (2019) The Optimization Design with Minimum Power for Variable Speed Control Moment Gyroscopes with Integrated Power and Attitude Control. *Aerospace Science and Technology*, **88**, 287-297. <https://doi.org/10.1016/j.ast.2019.03.028>
- [5] Richie, D.J., Lappas, V.J. and Palmer, P.L. (2007) Sizing/Optimization of a Small Satellite Energy Storage and Attitude Control System. *Journal of Spacecraft and Rockets*, **44**, 940-952. <https://doi.org/10.2514/1.25134>
- [6] Liu, F., Gao, Y. and Zhang, W. (2021) Large Angle Maneuver and High Accuracy Attitude Pointing Steering Law for Variable Speed Control Momentum Gyroscopes. *Journal of the Franklin Institute*, **358**, 3441-3469. <https://doi.org/10.1016/j.jfranklin.2021.02.019>
- [7] Yao, Y., Liu, F. and Zhao, H. (2016) Constrained Steering Law for VSCMGs with the Function of Attitude Control and Energy Storage. *Aerospace Science and Technology*, **58**, 341-350. <https://doi.org/10.1016/j.ast.2016.08.030>
- [8] Zhao, H., Liu, F. and Yao, Y. (2017) Optimization Design Steering Law for VSCMGs with the Function of Attitude Control and Energy Storage. *Aerospace Science and Technology*, **65**, 9-17. <https://doi.org/10.1016/j.ast.2017.02.005>
- [9] Kojima, H. (2013) Singularity Analysis and Steering Control Laws for Adaptive-Skew Pyramid-Type Control Moment Gyros. *Acta Astronautica*, **85**, 120-137. <https://doi.org/10.1016/j.actaastro.2012.12.019>
- [10] Yoon, H. and Tsotras, P. (2004) Singularity Analysis of Variable-Speed Control Moment Gyros. *Journal of Guidance, Control, and Dynamics*, **27**, 374-386. <https://doi.org/10.2514/1.2946>
- [11] MaMahon, J. and Schaub, H. (2009) Simplified Singularity Avoidance Using Variable Speed Control Moment Gyroscope Null Motion. *Journal of Guidance, Control, and Dynamics*, **32**, 1938-1943. <https://doi.org/10.2514/1.45433>
- [12] Jun, L. and Chao, H. (2007) Attitude Control of Large Angle Maneuver for Microsatellite Using Variable Speed Control Moment Gyros. *Chinese Journal of Space Science*, **27**, 336-341. <https://doi.org/10.11728/cjss2007.04.336>
- [13] Jia, Y.H. and Xu, S.J. (2007) Integrated Power and Attitude Control of Spacecraft Using Variable Speed Control Moment Gyros. *Chinese Journal of Aeronautics*, **28**, 647-653.
- [14] Jung, D. and Tsotras, P. (2007) An Experimental Validation of Spacecraft Attitude and Power Tracking with Variable Speed Control Moment Gyroscopes. *AAS Spaceflight Mechanics Meeting*, Sedona, January 2007, 7-130.
- [15] Zhang, J. and Xu, S.J. (2008) Singularity Analysis and Steering Law Design of IPACS with VSCMGs. *Chinese Journal of Aeronautics*, **29**, 123-130.
- [16] Zhang, J. and Xu, S.J. (2006) A Projection Matrix Approach for Design of IPACS of Spacecraft with VSCMGs. *Journal of Astronautics*, **27**, 609-615.
- [17] Jia, Y.H. and Xu, S.J. (2003) Study on Integrated Attitude/Power Control Using Variable Speed Control Moment Gyros. *Journal of Astronautics*, **24**, 32-37.

- [18] Fausz, J.L. and Richie, D.J. (2001) Flywheel Simultaneous Attitude Control and Energy Storage Using a VSCMG Configuration. *Proceedings of the 2000 IEEE International Conference on Control Applications*, Anchorage, 27 September 2001, 991-995.
- [19] Dominguez, J. and Wie, B. (2002) Computation and Visualization of Control Moment Gyroscope Singularities. *AIAA Guidance, Navigation, and Control Conference and Exhibit*. 2002: 4570.
- [20] Wie, B. (2004) Singularity Analysis and Visualization for Single-Gimbal Control Moment Gyro Systems. *Journal of Guidance, Control, and Dynamics*, **27**, 271-283. <https://doi.org/10.2514/1.9167>